Technical Notes

Analysis of Huygens Entry Observation to Inform Titan Shock-Layer Radiation Models

Christopher O. Johnston*
NASA Langley Research Center, Hampton, Virginia 23681
and
Aaron M. Brandis†
AMA Inc. at NASA Ames Research Center, Mountain View, California 94035

https://doi.org/10.2514/1.T6453

I. Introduction

THE Huygens probe entered Titan's atmosphere in 2005. As reviewed by Lorenz et al. [1], Earth-based telescopes attempted to measure the shock-layer radiation emitted during the probe's hypersonic entry phase. One of these attempts, reported by de Pater et al. [2], obtained radiation measurements over the region of Titan where the Huygens probe was descending. However, a noticeable shock-layer radiation component from the entering Huygens probe was not apparent in these measurements. The expected background signal from the Titan atmosphere indicated that the measurement device was working correctly. Lorenz et al. [1] showed in 2006, with optimistic assumptions [3,4], that a measurable shock-layer component might have been detectable above the measurement noise floor of 0.8 μJy (which in more familiar units to shock-layer radiation studies is 8.3×10^{-26} W/cm^2-nm at 1700 nm), with a predicted signal as high as 2.7 μJy. This unit of μJy, or micro-Jansky, is used here to be consistent with Lorenz et al. and de Pater et al. Since 2006, advances to the Titan radiation modeling capability have been made [5–8] for wake flows, where radiation simulations were previously not available [9]. Because the de Pater et al. measurements viewed the entry probe from roughly an angle of 30 deg from the rear, simulations of these measurements require accurate wake radiation modeling.

The goal of this Technical Note is to demonstrate that Titan radiation modeling advancements made since 2006 result in predictions of the de Pater et al. measurement far below the 0.8 μJy noise floor. This result provides the previously unavailable explanation for the lack of an observable shock-layer radiation signal. The motivation for demonstrating this consistency between the current state of the art and this measurement is to provide some level of experimental validation for Titan entry wake radiation predictions. This validation is currently of interest for the design of the Dragonfly mission [10], which is scheduled to land on Titan in the early 2030s. Although admittedly limited, the validation provided by this analysis is valuable because no other measurements capture emission from a representative Titan atmospheric entry in the recirculating wake flow environment. Based on current models, Johnston [9] shows that emission from this recirculating flow region should be negligible, with most of the backshell radiative heating for Dragonfly originating from the immediate post-shock flow within the field of view of the backshell surface. The present analysis provides the first experimental confirmation of this observation. This is an important finding, because if the modeling was erroneously underpredicting this separated wake flow radiation, the radiative heating to the backshell of Titan entry vehicles, such as Dragonfly [10], could be underpredicted.

Received 16 August 2021; revision received 5 October 2021; accepted for publication 6 October 2021; published online 3 November 2021.

*Aerospace Engineer, Aerothermodynamics Branch; christopher.o.johnston@nasa.gov. Associate Fellow AIAA.

†Senior Research Scientist, Aerothermodynamics Branch. Associate Fellow AIAA.

II. Measurement Details

The night sky was clear in Hawaii when Huygens entered Titan, which made possible the de Pater et al. [2] measurement from the Keck II Observatory. A NIRC2 camera was used with a methane band filter, which measured wavelengths in the 1610–1740 nm range, where the measured radiative flux is the average within this range. Note that only a small fraction of the cyanogen (CN) red band, which dominates the backshell radiation for Titan entry vehicles, is captured in this wavelength range. However, the primary uncertainty in the CN red model is the upper electronic state population, which impacts the entire band equally. Therefore, the validation provided by the present analysis may be assumed to apply over the entire band system.

The 1610–1740 nm wavelength range is essentially transparent above an altitude of 150 km at Titan for radiation directed outward [11], which covers the peak heating range of the Huygens probe. Below this altitude, Titan's atmosphere is opaque in this wavelength range, which is advantageous for the shock-layer radiation measurements at the altitudes of interest because this provides a dark background for the Earth-based measurement. The Earth's atmosphere is also essentially transparent in this wavelength range [12], so atmospheric absorption in both Earth's and Titan's atmosphere is ignored in this analysis. The measurements were taken in 10 s intervals. As mentioned in the Introduction, no shock-layer radiation component was seen during the Huygens probe entry, therefore implying that the shock-layer emission in the 1610–1740 nm range, directed back to Earth, was below the 0.8 μJy measurement noise floor.

III. Simulation Details

The flowfield simulation approach applied in this work is summarized by Johnston et al. [9]. The flowfield is modeled using the LAURA finite-volume, Navier–Stokes flow solver [13]. A two-temperature thermochemical nonequilibrium model [14] is applied based on a modified Gökçen [15] rate model. These simulations apply the following 20 species: CH_4, CH_3, CH_2, CH, N_2, C_2, H_2, CN, C_2N_2, NH, HCN, N, C, H, N_2^+, CN^+, N^+, C^+, H^+, and e^-. This approach includes a number of advancements relative to the mid-2000s' models applied in the simulations used by Lorentz et al. [1] to conclude that predicted signal as high as 2.7 μJy should be seen. The primary advancements are the application of a non-Boltzmann model for the radiating levels of CN, which allows the Boltzmann assumption to be removed, and the application of a ray-tracing model for the radiative transfer, which allows the radiative flux emitted from the shock-layer in the direction of Earth to be computed in detail. The non-Boltzmann model has been compared with shock-tube measurements and shown to provide significantly better predictions than the Boltzmann model [9], with the Boltzmann model overpredicting the experimental data by up to an order of magnitude. Other minor improvements include the addition of C_2N_2 and modification of the $CN + H_2 \leftrightarrow HCN + H$ rate listed by Gökçen.

Table 1 Huygens freestream conditions considered in this work

Time, s	Velocity, m/s	Density, kg/m^3	Temp., K
184	5410	1.76×10^{-4}	182
187	5162	2.28×10^{-4}	182
191	4775	3.18×10^{-4}	182

The freestream conditions considered for the present simulations are focused on the peak radiative heating conditions, which will provide the largest possible signal, and are therefore the most likely to have exceeded the 0.8 μJy limit. Table 1 lists these peak radiative heating conditions, which cover an 8 s period of the trajectory. These conditions are based on the postflight correction to the atmospheric model, which are listed as the "Post-Ta" cases by Caillault et al. [3]. Also taken from the postflight analysis are the freestream mass fractions, which for N_2 and CH_4 are 0.9896 and 0.0104, respectively. Although simulations for vehicle design may assume larger amounts of CH_4 to assure conservatism for CN radiation, the present analysis applies the nominal best estimate for the CH_4 mass fraction.

Once the flowfield simulation is obtained, the radiative flux from the shock layer to the observer is computed as a postprocessing step. Figure 1 illustrates the rays that are interpolated through the flowfield at a 30 deg observation angle appropriate for the Huygens observations [1]. The five rays shown in this figure are illustrative, as the actual calculation considers over 6000 rays, which were chosen to fully resolve the intensity distribution. Along each of these lines the radiative intensity is computed. The right-hand frame of Fig. 2 shows the resulting distribution of the radiative intensity projected onto the two-dimensional viewing plane defined in Fig. 1. The spatial integral over this viewing plane, which is then divided by the distance from the viewing plane to the Earth observation station squared, provides the total radiative flux. Note that the distance between the Huygens probe and the measurement was assumed equal to 1.28×10^9 km. Whereas Fig. 2 considers the entire spectral range between 1600–1750 nm, the same spatial integration is applied individually to each spectral point to produce the observed spectrum. Shock-layer radiation spectra are typically computed in units of W/cm^2-nm. These units are converted to μJy through the following conversion [16]:

$$q_{\text{obs}}(\mu\text{Jy}) = 3.3 \times 10^{18} \times [q_{\text{obs}}(\text{W/cm}^2\text{-nm})] \times [\lambda(\text{nm})]^2 \qquad (1)$$

These units of μJy will be applied for the remainder of the simulations applied in this work.

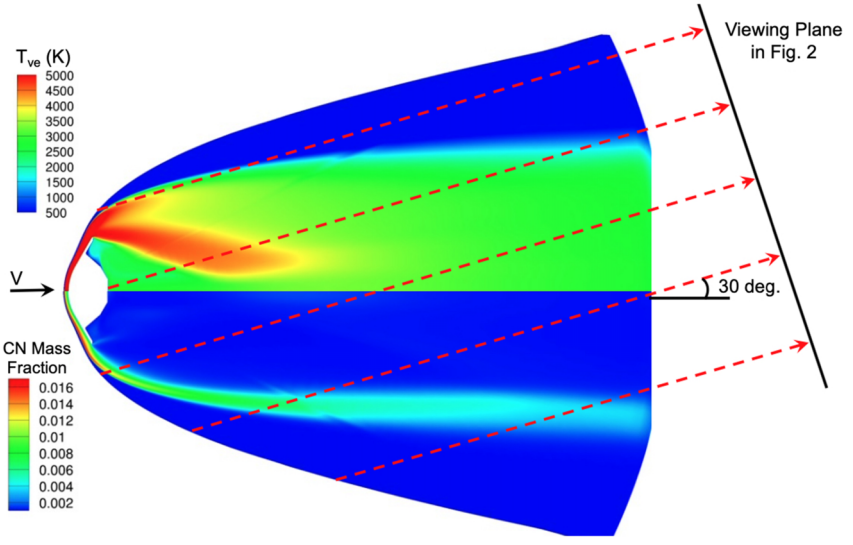

Fig. 1 Schematic of the ray-tracing radiation simulation for the observed radiative flux.

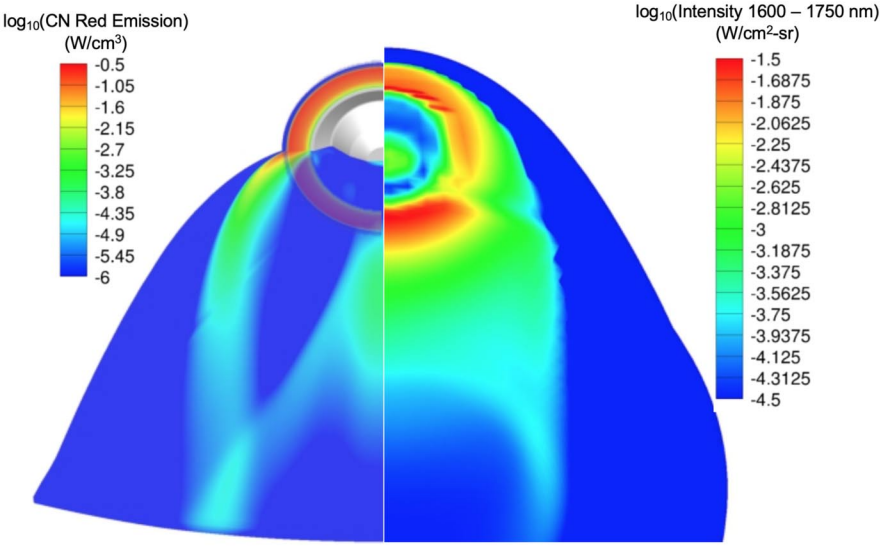

Fig. 2 Flowfield distribution of the CN-red band emission and the resulting intensity distribution for the 187 s case as seen from the actual view angle.

IV. Results and Discussion

The simulated radiative flux spectra of the Earth-based measurements are presented in Fig. 3 for the three trajectory points listed in Table 1. Note that the narrow peaks below 500 nm represent the CN violet band, whereas the spectrum above 500 nm is dominated by the CN red band. The measurement range between 1610 and 1740 nm is therefore dominated by CN red, which contributes over 98% of the radiative flux in this range. The simulated radiative flux levels in the measured wavelength range are less than 0.01 μJy, which is nearly two orders of magnitude below the measurement noise floor of 0.8 μJy. These simulations are therefore in agreement with lack of a measurable signal reported by de Pater et al. [2]. This result is in contrast to the 2006-era result reported by Lorenz et al. [1], as mentioned in the Introduction. The present values are significantly lower than those predicted by Lorenz et al. for two reasons. The first is that the present simulations apply a non-Boltzmann model for CN, which results in its decreased emission. This non-Boltzmann model has been shown to provide significantly better comparisons with shock-tube measurements than the Boltzmann assumption. Second, the radiative intensity directed from the wake behind the capsule toward Earth is computed in detail, as shown in Figs. 1 and 2. This ray-tracing approach allows the geometric approximations applied by Lorenz et al. to be avoided, which assumed stagnation-line emission emitted over a 7 m^2 area representative of the heatshield dimensions. This advancement is important, because the wake emission captured by the ray-tracing approach is significantly lower than the stagnation-line emission.

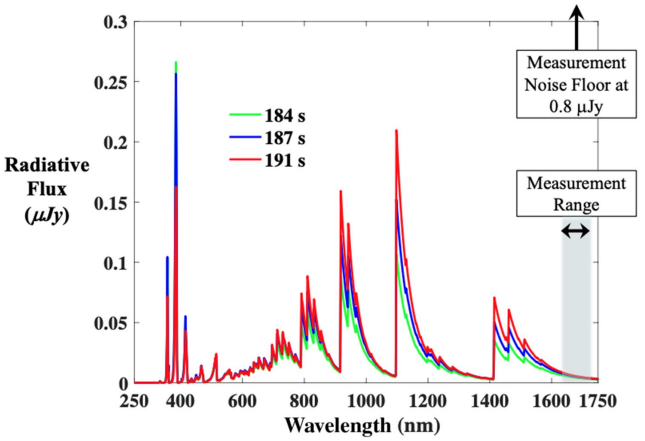

Fig. 3 Summary of simulated observed radiation spectra for Huygens.

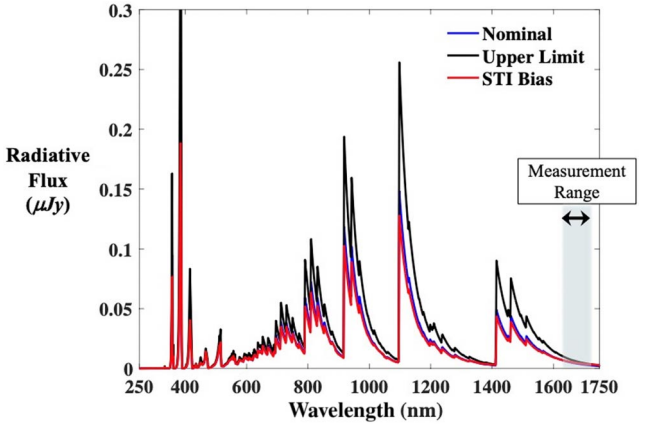

Fig. 4 Uncertainty of the simulated radiation for $t = 187$ s.

The upper-limit uncertainty for the 187 s simulation was computed using the parametric uncertainties defined in Johnston et al. [9]. The comparison between the nominal and upper-limit spectrum is presented in Fig. 4. In the 1610–1740 nm range, the upper-limit uncertainty is roughly 50% above the nominal, which is far from the nearly two order of magnitude increase required to reach the 0.8 μJy detection limit. Also shown in the figure is the shock-tube informed bias (STI bias) result, which essentially maps the NASA Ames electric arc shock tube (EAST) measurements from Brandis and Cruden [7] to the simulation flowfield [17]. This STI bias result for the Huygens observation is 17% lower than the nominal simulation, which is below the 0.8 μJy detection limit. These upper-limit uncertainty and STI bias results confirm that the 0.8 μJy value is beyond the justifiable simulation uncertainty bounds.

It is informative to show the relevance of the present simulations to the radiative heating of the Dragonfly capsule currently being designed. Figures 5 and 6 compare the grouped contribution of temperatures and non-Boltzmann ratio (for CN red) between the Huygens observed (or directed away from the capsule) radiative flux and Dragonfly surface radiative flux, both considering only radiation between 1600 and 1750 nm. The backshell surface point near the forebody shoulder is considered for the Dragonfly case at the peak radiative heating condition [10]. These figures are produced by differentiating the radiative intensity along each ray of the ray-tracing computation and placing this change in the radiative intensity, weighted by the solid angle of the ray, into its appropriate temperature or non-Boltzmann ratio group. Note that the bar graph components sum to one in each figure. Figure 5 shows that most of the radiation for both cases originates from flowfield regions between 5000 and 7000 K. Similarly, Fig. 6 shows that both cases contain significant non-Boltzmann emission for CN red, with the average ratio between the non-Boltzmann and Boltzmann populations roughly equal to 0.5 for both the Huygens and Dragonfly cases. Although these distributions are not exactly the same between the Huygens and Dragonfly cases, the similarity provides evidence that the limited experimental validation provided by the Huygens comparison may be leveraged for Dragonfly design. Note that, by definition, experimental valida-

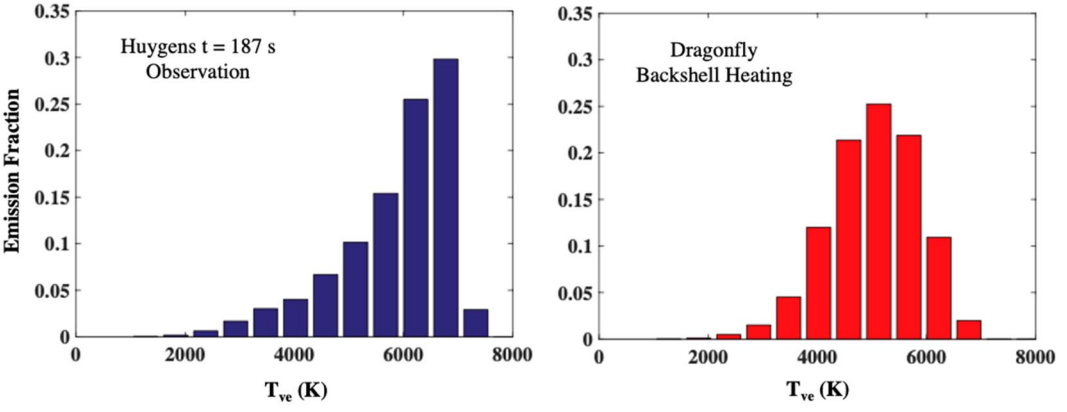

Fig. 5 Comparison of the flowfield temperature contributions to the simulated radiation between Huygens observation and Dragonfly backshell surface point between 1610 and 1740 nm.

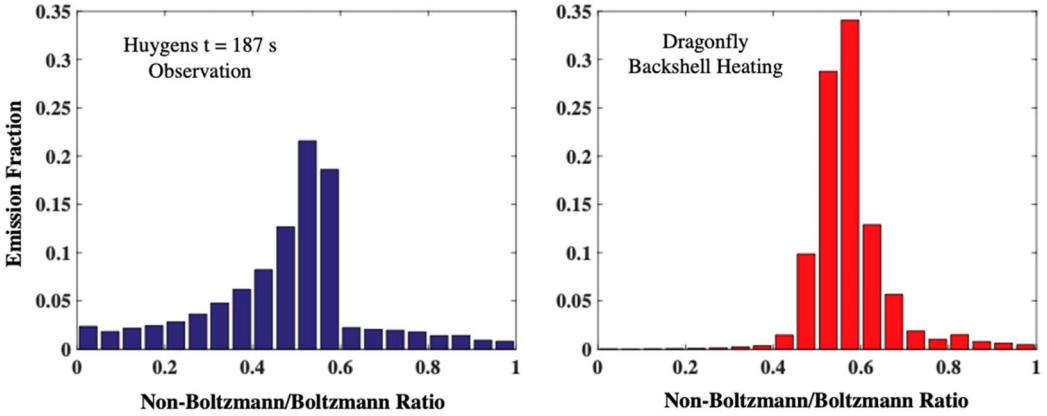

Fig. 6 Comparison of the non-Boltzmann ratio contributions to the simulated radiation between Huygens observation and Dragonfly backshell surface point between 1610 and 1740 nm.

tion requires determining the discrepancy between the simulation and measurement, which is not entirely possible with the current case because no quantitative measurements are available. However, by assuming the conservative limit that the actual radiative flux was just below the measurement noise floor, then showing that the simulations are below this measurement noise floor by two orders of magnitude eliminates the possibility that the simulations underpredict the measurement by more than two orders of magnitude. In other words, the upper-limit uncertainty (or margin) on the simulated wake radiation should be less than two orders of magnitude based on this comparison. This does not mean that the upper-limit uncertainty of the wake radiation is two orders of magnitude, only that it is less than two orders of magnitude, which is consistent with the STI bias and parametric uncertainty results presented in Fig. 4.

V. Conclusions

Radiation during the Huygens hypersonic entry was monitored in the 1610–1740 nm wavelength range by Earth-based instruments. Shock-layer radiation simulations from 2005 suggested that the shock-layer radiation from Huygens should be seen above the noise floor of these measurements. However, a noticeable signal from shock-layer radiation was not apparent in the resulting Huygens measurements. This work shows that shock-layer advancements made since 2005, which include non-Boltzmann modeling, ray-tracing radiative transport, and shock-tube informed bias result in a simulated radiative flux far below the measurement noise floor. These simulations are therefore consistent with the measurement. This consistency provides a level of flight data validation for the wake radiation for a Titan entry vehicle, which is otherwise unavailable. In its most conservative interpretation, this comparison implies that the upper-limit uncertainty in the wake radiation is less than two orders of magnitude, and likely much less based on parametric uncertainty and STI bias analyses. This limited validation is useful for assessing the backshell radiative heating to the Dragonfly capsule, which is currently being designed for Titan entry.

References

[1] Lorenz, R. D., Witasse, O., Lebreton, J. P., Blancquaert, T., de Pater, I., Mazoue, F., Roe, H., Lemmon, M. T., Burratti, B. J., Holmes, S., and Noll, K., "Huygens Entry Emission: Observation Campaign, Results, and Lessons Learned," *Journal of Geophysical Research*, Vol. 111, No. E07S11, 2006. https://doi.org/10.1029/2005 JE002603

[2] de Pater, I., Adamkovics, M., Bouchez, A. H., Brown, M. E., Gibbard, S. G., Marchis, F., Roe, H. G., Schaller, E. L., and Young, E., "Titan Imagery with Keck Adaptive Optics During and After Probe Entry," *Journal of Geophysical Research*, Vol. 111, No. E07S05, 2006. https://doi.org/10.1029/2005 JE002620

[3] Caillault, L., Walpot, L. M., Magin, T. A., Bourdon, A., and Laux, C. O., "Radiative Heating Predictions for Huygens Entry," *Journal of Geophysical Research*, Vol. 111, No. E09S90, 2006. https://doi.org/10.1029/2005 JE002627

[4] Walpot, L. M., Caillault, L., Molina, R. C., Laux, C. O., and Blanquaert, T., "Uncertainty Analysis of Radiative Heating Predictions for Titan Entry," *Journal of Thermophysics and Heat Transfer*, Vol. 20, No. 4, 2006, pp. 663–671. https://doi.org/10.2514/1.20901

[5] Brandis, A. M., Morgan, R. G., McIntyre, T. J., and Jacobs, P. A., "Nonequilibrium Radiation Intensity Measurements in Simulated Titan Atmospheres," *Journal of Thermophysics and Heat Transfer*, Vol. 24, No. 2, 2010, pp. 291–300. https://doi.org/10.2514/1.44482

[6] Brandis, A. M., Morgan, R. G., and McIntyre, T. J., "Analysis of Non-equilibrium CN Radiation Encountered During Titan Atmospheric Entry," *Journal of Thermophysics and Heat Transfer*, Vol. 25, No. 4, 2011, pp. 493–499. https://doi.org/10.2514/1.50966

[7] Brandis, A. M.., and Cruden, B. A., "Titan Atmospheric Entry Radiative Heating," AIAA Paper 2017-4534, 2017. https://doi.org/10.2514/6.2017-4534

[8] Magin, T. E., Caillault, L., Bourdon, A., and Laux, C. O., "Nonequilibrium Radiative Heat Flux Modeling for the Huygens Entry Probe," *Journal of Geophysical Research*, Vol. 111, No. E07S12, 2006, https://doi.org/10.1029/2005 JE002616

[9] Johnston, C. O., West, T., and Brandis, A., "Features of Afterbody Radiative Heating for Titan Entry," AIAA Paper 2019-3010, 2019, https://doi.org/10.2514/6.2019-3010

[10] Brandis, A. M., Saunders, D., Allen, G., Stern, E., Wright, M., Johnston, C. O., Adams, D., and Lorenz, R., "Aerothermodynamics for Dragonfly's Titan Entry," *15th International Planetary Probe Workshop (IPPW)*, Boulder, CO, 2018.

[11] Maltagliati, L., Bezard, B., Vinatier, S., Hedman, M. M., Lellouch, E., Nicholson, P. D., Sotin, C., de Kok, R. J., and Sicardy, B., "Titan's Atmosphere as Observed by Cassini/VIMS Solar Occultations: CH_4, CO and Evidence for C_2H_6 Absorption," *Icarus*, Vol. 248, March 2015, pp. 1–24. https://doi.org/10.1016/j.icarus.2014.10.004

[12] Berk, A., Anderson, G. P., Acharya, P. K., Bernstein, L. S., Muratov, L., Lee, J., Fox, M., Adler-Golden, S. M., Chetwynd, J. H., Hoke, M. L., Lockwood, R. B., Gardner, J. A., Cooley, T. W., Borel, C. C., and Lewis, P. E., "MODTRAN 5: A Reformulated Atmospheric Band Model with Auxiliary Species and Practical Multiple Scattering Options: Update," *Algorithms and Technologies for Multispectral, Hyperspectral, and Ultraspectral Imagery XI*, SPIE, 2005.

[13] Mazaheri, A., Gnoffo, P. A., Johnston, C. O., and Kleb, B., "Laura Users Manual: 5.5-76679," NASA TM 217800, May 2017.

[14] Gnoffo, P. A., Gupta, R. N., and Shinn, J. L., "Conservation Equations and Physical Models for Hypersonic Air Flows in Thermal and Chemical Nonequilibrium," NASA TP 2867, Feb. 1989.

[15] Gocken, T., "N_2–CH_4–Ar Chemical Kinetic Model for Simulations of Atmospheric Entry to Titan," *Journal of Thermophysics and Heat Transfer*, Vol. 21, No. 1, 2007, pp. 9–18. https://doi.org/10.2514/1.22095

[16] Wilkins, G. A., "The IAU Style Manual," *IAU Transactions XXB*, IAU, 1989.

[17] Johnston, C. O., "Evaluating Shock-Tube Informed Biases for Shock-Layer Radiative Heating Simulations," *Journal of Thermophysics and Heat Transfer*, Vol. 35, No. 2, 2021, pp. 349–361. https://doi.org/10.2514/1.T6174